Paper:

Bezodis, N. Phase analysis in maximal sprinting: an investigation of step-to-step technical changes between the initial acceleration, transition and maximal velocity phases. *Sports Biomechanics*
http://dx.doi.org/10.1080/14763141.2018.1473479

_Title: Phase analysis in maximal sprinting: an investigation of step-to-step technical changes between the initial acceleration, transition and maximal velocity phases.

Authors:
Hans C. von Lieres und Wilkau[1], Gareth Irwin[1], Neil E. Bezodis[2], Scott Simpson[3], Ian N. Bezodis[1]

Cardiff School of Sport and Health Sciences, Cardiff Metropolitan University, Cardiff, Wales, UK[1]
Applied Sports, Technology, Exercise and Medicine Research Centre, Swansea University, Swansea, Wales, UK[2]
Welsh Athletics, Cardiff, Wales, UK[3]

Correspondence:
Hans C. von Lieres und Wilkau, Cardiff School of Sport and Health Sciences, Cardiff Metropolitan University, Cardiff, Wales, UK. E-mail: havonlieres@cardiffmet.ac.uk, Telephone number: 029 2020 5027.

Co-authors:
Gareth Irwin, Cardiff School of Sport and Health Sciences, Cardiff Metropolitan University, Cardiff, Wales, UK. girwin@cardiffmet.ac.uk, Telephone number: 029 2041 7274.

Neil E. Bezodis, Applied Sports, Technology, Exercise and Medicine Research Centre, Swansea University, Swansea, Wales, UK. n.e.bezodis@swansea.ac.uk, Telephone number: (01792) 295801.

Scott Simpson, Welsh Athletics, Cardiff, Wales, UK, scott.simpson@welshathletics.org, Telephone number: 029 2020 1520.

Ian N. Bezodis, Cardiff School of Sport and Health Sciences, Cardiff Metropolitan University, Cyncoed Road, Cardiff, Wales, UK. ibezodis@cardiffmet.ac.uk, 029 2041 7245.

Acknowledgements:
The authors are grateful to Melanie Golding, Laurie Needham, Adam Brazil and James Cowburn for their assistance with data collection, and to the coach and athletes who participated in this study.

Funding:
This work was supported by Welsh Athletics, Sport Wales and the Cardiff School of Sport and Health Sciences.

Abstract

The aim of this study was to investigate spatiotemporal and kinematic changes between the initial acceleration, transition and maximum velocity phases of a sprint. Sagittal plane kinematics from five experienced sprinters performing 50 m maximal sprints were collected using six HD-video cameras. Following manual digitising, spatiotemporal and kinematic variables at touchdown and toe-off were calculated. The start and end of the transition phase were identified using the step-to-step changes in centre of mass height and segment angles. Mean step-to-step changes of spatiotemporal and kinematic variables during each phase were calculated. Firstly, the study showed that if sufficient trials are available, step-to-step changes in shank and trunk angles might provide an appropriate measure to detect sprint phases in applied settings. However, given that changes in centre of mass height represent a more holistic measure, this was used to sub-divide the sprints into separate phases. Secondly, during the initial acceleration phase large step-to-step changes in touchdown kinematics were observed compared to the transition phase. At toe-off, step-to-step kinematic changes were consistent across the initial acceleration and transition phases before plateauing during the maximal velocity phase. These results provide coaches and practitioners with valuable insights into key differences between phases in maximal sprinting.

Key Words: acceleration phase; kinematics; sprint technique; coaching

Introduction

The sprint running events have traditionally been sub-divided into acceleration, constant velocity and deceleration phases (e.g. Volkov & Lapin, 1979). Due to the multidimensional structure of the acceleration phase (Delecluse, 1997), the scientific (e.g. Delecluse, Van Coppenolle, Willems, Diels, Goris, Van Leemputte & Vuylsteke, 1995; Nagahara, Matsubayashi, Matsuo & Zushi, 2014b) and coaching (e.g. Dick, 1987; Seagrave, 1996; Crick, 2014a) literature have further sub-divided the acceleration phase. For the purposes of this paper, the naming convention used by Delecluse et al. (1995) will be adopted, where the first and second acceleration phases will be referred to as the initial acceleration phase and the transition phase, respectively. The transition phase is then followed by the maximal velocity phase.

With performance-related factors differing between the phases in a sprint, Delecluse, Van Coppenolle, Diels and Goris (1992) suggested that a good performance in one phase does not guarantee good performance in other phases. An increased understanding of the characteristics of the different phases in sprinting can provide important insights for coaches and applied sport scientists of the changes in mechanics between phases of a maximal sprint. However, with the specific length of each phase dependent on the athletes' ability (Delecluse, 1997), it is challenging to tailor training sessions to individual athletes. Recently, scientific (e.g. Nagahara et al., 2014b) and coaching literature (e.g. Crick, 2014a) identified the use of step-to-step progressions of postural measures to identify phases in maximal sprinting.

Using the step-to-step changes of the centre of mass height (CM-h), Nagahara et al. (2014b) identified two breakpoint steps (approximately steps 4 and 14) which were used to subdivide the sprint into three phases. Distinct changes were reported in spatiotemporal and kinematic variables (Nagahara et al., 2014b) and external kinetics (Nagahara, Mizutani & Matsuo, 2016; Nagahara, Mizutani, Matsuo, Kanehisa & Fukunaga, 2017a) as sprinters crossed from one phase to the next. Similarly, coaching literature proposed that step-to-step progressions of shank and trunk angles at touchdown are specific to each phase of a maximal sprint (Crick, 2014a). It is suggested that the initial acceleration phase ends when step-to-step changes in shank angles end as the shank becomes perpendicular to the ground at touchdown (suggested to be: steps 5-7; Crick, 2014b), while the transition phase ends when step-to-step changes in trunk angle cease as the trunk becomes upright (suggested to be: step 17; Crick, 2014c). However, considering that changes in CM-h represent a holistic measure of whole-body changes it is unknown whether the first and second acceleration phases identified by Nagahara et al. (2014b) will align with the initial acceleration and transition phases described by Crick (2014a). This may have important practical implications to ensure the appropriate alignment of information that is shared between researchers, coaches and applied sport scientists.

Performance during sprint acceleration depends on the net anteroposterior force generated during ground contact, which directly influences the anteroposterior centre of mass (CM) acceleration (Rabita, Dorel, Slawinski, Sàez de Villarreal, Couturier, Samozino & Morin, 2015). Theoretically, the orientation of the sprinter (i.e. the vector connecting the sprinter's CM to the contact point with the ground (CM-angle) is mechanically related to their acceleration (di Prampero, Fusi, Sepulcri, Morin, Belli & Antonutto, 2005). As sprinters assume a more forward-inclined CM-angle during the initial acceleration phase, anteroposterior CM acceleration is larger compared with the later phases of a sprint when sprinters adopt a less forward-inclined posture. However, the CM-angle depends on both the CM-h and the anteroposterior distance between the contact point and the CM, which in turn are dependent on the orientation of the segments of the stance leg and trunk. Thus, knowledge of the step-to-step changes in segment angles of the stance leg and trunk are important to understand how sprinters' orientation and CM acceleration changes to address the requirements of the different sprint phases.

An understanding of the evolution whole-body posture and segment orientations during acceleration can have important implications for developing technical models of sprinting and informing technical interventions. Therefore, the aim of this study was to investigate spatiotemporal and kinematic changes between the initial acceleration, transition and maximum velocity phases of a sprint. Two research questions were formulated; the first research question – '*how comparable are the sprint acceleration phases when identified using different measures?'* aimed to compare and critically appraise the use of either CM-h (Nagahara et al., 2014b) or shank and trunk angles (Crick, 2014a) to identify breakpoint steps in sprint acceleration. The second research question – '*how do step-to-step progressions of spatiotemporal and kinematic variables differ between the initial acceleration, transition and maximal velocity phases?*' aimed to characterise the technical changes throughout a maximal sprint. It was hypothesised that; a) the sprint acceleration phases identified using changes in CM-h will align with the phases identified using shank and trunk angles and b) there will be large differences in step-to-step changes of the orientation of sprinters (i.e. CM-angle) between the initial acceleration, transition and maximal velocity phases.

Methods

Participants and procedures

Following institutional ethical approval, three male and two female national-level sprinters (Table 1) gave written informed consent to participate. Data were collected in March (after the indoor season) and eight weeks later in May (early outdoor season) during participants' regular training sessions.

****Insert table 1 near here****

Prior to data collection, the participants performed a coach-led warm-up. The warm-up incorporated; dynamic stretching, sprint specific drills, and was concluded with 3-5 runs of increasing intensity. The participants then performed up to three practice starts from the starting blocks, before commencing with the data collection. Following the warm-up, data were collected from five maximal 50 m sprints from blocks, with at least five minutes rest between trials to ensure a full recovery. One sprinter (P3) only completed three sprints at the second collection. Each sprint was started with *'on your marks'* and *'set'* commands, followed by a manually triggered auditory starting signal. All participants wore sprinting shoes and the testing was done on a Mondo track surface.

Data collection set-up

Five HDV digital cameras (1×Sony Z5; 2×Sony Z1; 2×Sony A1E, Sony, Tokyo, Japan) were mounted on tripods at a height of 1.80 m and 19 m from the running lane (Cameras 1 – 5; Figure 1). The cameras recorded in HD (1440 × 1080 pixels) at 50 Hz with an open iris and a shutter speed of 1/600 s.

****Insert figure 1 near here****

A sixth camera (Sony Z5) was set up perpendicular to the 25 m mark and 40 m away from the running lane was panned during trials and used to identify touchdown and toe-off events. It recorded in HD (1440 × 1080 pixels) at 200 Hz with an open iris and a shutter speed of 1/600 s. Two sets of 20 sequentially illuminating LEDs (Wee Beastie Electronics, Loughborough, UK), which were synchronised to the starting signal, were used to synchronise cameras 1 to 4 with the 200 Hz panning camera to within 0.001 s (Irwin & Kerwin, 2006). Camera 5 was subsequently synchronised to camera 4 through calculation of a time offset, which was based on the participants' CM position data from the overlap between cameras 4 and 5. First, the time difference between cameras 4 and 5 was determined. Using linear interpolation between two successive CM positions (0.020 s apart) from camera 4, the time at the closest corresponding CM position from camera 5 was estimated. Secondly, the time difference between cameras 4 and 5 was added to the camera 4's synchronisation data from the LED synchronisation lights. This provided the necessary timing data needed to synchronise camera 5 with the 200 Hz panning camera.

Data reduction

Videos were manually digitised in Matlab (The MathWorks Inc., USA, version R2014a) using an open source package (DLTdv5, Hedrick, 2008). The data required for calibration was obtained by digitising recordings of a vertical calibration pole with three spherical control points (diameter of 0.100 m) which was moved sequentially through three to five known locations across each camera's field of view (Figure 1). This allowed a 10.00 m × 2.17 m plane to be calibrated for cameras 1 to 5 using an open source eight parameter 2D-DLT (Meershoek, 1997) which was edited to include a ninth parameter to account for lens distortion (Walton, 1981). The accuracy of spatial reconstruction was assessed by calculating horizontal and vertical root-mean-squared differences (RMSD) between reconstructed and known points within the calibrated plane. Across both days, reconstruction errors were suitably low, ranging from 0.002 - 0.005 m.

From the panning camera videos, the touchdown and toe-off events were identified. Touchdown was defined as the first frame when the foot was visibly on the ground, while toe-off was defined as the first frame when the foot was visibly off the ground. The identification of touchdown and toe-off was repeated three times for each trial with at least five days between repetitions. The events identified consistently on at least two separate occasions were used in subsequent processing as the touchdown and toe-off events. Static camera videos were digitised for two frames around each touchdown (last frame before and the first frame of ground contact) and toe-off (last frame before and the first frame of flight) (Bezodis, Kerwin & Salo, 2008). Sixteen body landmarks were digitised: vertex and seventh cervical vertebra (C7), then both hips, shoulders, elbows, wrists, knees, ankles and metatarsophalangeal (MTP) joint centres. Furthermore, the distal end of the contact foot (i.e. the toe) was digitised for three consecutive frames while the foot was on the ground. These three consecutively digitised frames were later averaged during data processing to provide a measure for the position of the front of the shoe during ground contact. To better approximate spatiotemporal data at touchdown and toe-off, event times from the 200 Hz panning camera were synchronised to the data from the static cameras using the LED synch lights (Figure 1) or a least squares fit to the touchdown and toe-off events. Overall, data from all cameras could be synchronised to the nearest 0.002 s. The coordinate positions of each of the digitised points at the 200 Hz touchdown and toe-off events were calculated via linear interpolation between the two frames digitised around touchdown and toe-off.

To evaluate the reliability of digitising, one trial was re-digitised three times. Variables of interest were calculated from the three sets of digitisations. The absolute and relative (expressed as a percentage of the absolute RMSD relative to variables range across the trial)

RMSDs between all re-digitisations were calculated for the variables measured. A relative RMSD below 5% was selected as a cut-off for a variable to be deemed reliable. The reliability analysis revealed acceptably low uncertainties with RMSDs of 0.03 $m \cdot s^{-1}$ (relative RMSD: 0.6%) for step velocity, between 0.005 - 0.010 m (relative RMSD: 0.0% - 2.9%) for height and distance variables, 0.02 Hz (relative RMSD: 2.0%) for step frequency and between 1° - 2° (relative RMSD: 0.8% - 3.9%) for angular variables. The reliability of the variables was therefore deemed acceptably low to identify step-to-step changes during the sprinting trials.

Data processing

The CM at touchdown and toe-off was calculated using segmental inertia data from de Leva (1996) apart from the foot segment for which Winter's (2009) data were used, with the added mass of each athlete's running shoe. Event times, and CM and joint centre locations at touchdown and toe-off were used to calculate the following variables:

Sprint Performance [s]: Time at 50 m minus reaction time. The 50 m time was calculated as the time when the participants' CM reached 50 m, using a fourth-order polynomial, which was fit through all consecutive touchdown and toe-off CM locations from step 1 onwards. Reaction time was determined from the 200 Hz panning camera as the moment when the participants showed the first visible movement in the starting blocks following the start signal.

Spatiotemporal variables: A step was defined from touchdown to the subsequent contralateral touchdown. Step velocity (m/s) was the anteroposterior CM displacement between two consecutive touchdowns divided by the time between the touchdown events. Step length (m) was the anteroposterior displacement of the CM between two consecutive touchdowns, while step frequency (Hz) was the inverse of step time from the panning camera touchdown events.

Contact time (s) was calculated by subtracting the touchdown time from the subsequent toe-off time. Flight time (s) was calculated by subtracting the toe-off time from the subsequent touchdown time. Contact distance (m) was calculated as the difference between the anteroposterior positions of the CM at touchdown and subsequent toe-off. Touchdown distance (TD distance, m) was the anteroposterior distance between the MTP and CM at touchdown while toe-off distance (TO distance, m) was the anteroposterior distance between the CM at toe-off and the average toe position during contact. Negative touchdown and toe-off distances represented the CM in front of the contact point. The flight distance (m) was calculated by subtracting the CM position at touchdown from the CM position at the preceding toe-off event.

Kinematics: Segment angles [°] were defined between the horizontal forward line and the vector created from the distal to proximal segment endpoints. CM, trunk (θ_{trunk}), thigh (θ_{thigh}) and shank (θ_{shank}) angles at touchdown and toe-off were calculated.

Data from each camera were combined into the full 50 m sprint trial. Since all participants performed at least 25 steps within the 50 m sprint, steps 1-25 were analysed further.

Phase identification

Phase identification was based on identifying breakpoint steps at the start of transition (T_{start}) and maximal velocity (MV_{start}) phases, respectively. The initial acceleration phase occurred between step one and the step preceding T_{start}, while the transition phase occurred between T_{start} and the step preceding MV_{start}. The maximal velocity phase was defined from MV_{start} to step 25. It must be acknowledged that this study will define the maximal velocity phase based on kinematic characteristics generally associated with this phase of the events (i.e. upright posture; e.g. Crick. 2014c) and therefore running velocity may show a small change during this phase. In order to address the first research question, T_{start} and MV_{start} were both identified using multiple approaches.

T_{start}: This breakpoint step was identified from step-to-step increases in touchdown CM-h (TD CM-h) and touchdown shank angle (TD shank angle). Based on previous literature (e.g. Delecluse et al., 1995; Nagahara et al., 2014b; Crick, 2014b), T_{start} was predicted to occur within the first 10 steps. Therefore, to remove the influence of subsequent data, only the first 10 steps of the sprint were used. A modified method involving multiple straight-line approximation was used to identify T_{start} (see Nagahara et al., 2014b for further details).

MV_{start}: This breakpoint step was identified based on step-to-step increases in TD CM-h and touchdown trunk angle (TD trunk angle). To remove the influence of data points from the start of the trial, only data from step eight onwards were used (Nagahara et al., 2014b). A method using two first order polynomials was used to identify MV_{start} (see Nagahara et al., 2014b for further details).

Data analysis

To address the first research question, and identify breakpoints during maximal sprint acceleration, all trials from both days were used. This allowed a more robust and thorough comparison of the measures used to subdivide the acceleration phase across a range of athletes, trials and sessions. The differences in T_{start} (calculated using either TD CM-h or TD shank angle) and MV_{start} (calculated using either TD CM-h or TD trunk angle) were quantified by calculating an RMSD between respective measures for each participant on each day.

To address the second research question, each participant's best trial from each day was selected based on 50 m times. This allowed the investigation of the step-to-step technical changes associated with only the best performances from each sprinter in the sample. The measure identified as 'most appropriate' from research question 1 was then used to identify T_{start} and MV_{start} breakpoint steps to address research question 2. T_{start} and MV_{start} breakpoint steps identified from the best trials were used to identify the steps occurring in the initial acceleration, transition and maximal velocity phases of the most successful sprints. Following the identification of T_{start} and MV_{start}, the step-to-step data profiles were smoothed using a Hanning three-point moving averages algorithm (Grimshaw, Fowler, Lees & Burden, 2004).

Mean step-to-step changes across the steps within the initial acceleration (IAP), transition (TP) and maximal velocity phases (MVP) were calculated for each variable, across each trial. Magnitude-based inferences (MBI; Batterham & Hopkins, 2006) were used to quantify meaningful differences between each participants' mean step-to-step changes between the phases. Differences between means (phases: TP-IAP; MVP-IAP; MVP-TP) were calculated using the post-only crossover spreadsheet (Hopkins, 2006) with a confidence interval (CI) of 97%. The smallest worthwhile change was an effect size of 0.2 (Hopkins, 2004; Winter, Abt & Nevill, 2014). Effect sizes were quantified using the following scale: <0.19 (trivial), 0.20-0.59 (small), 0.60-1.19 (moderate), 1.20-1.99 (large), 2.00-3.99 (very large) and >4.00 (extremely large; Hopkins, Marshall, Batterham & Hanin, 2009). The probability (percentage and qualitative description) that the differences were larger than 0.20 was defined as; possibly 25-75% (*); likely: 75-95% (**); very likely: 95-99.5% (***) and most likely >99.5% (****; Hopkins et al., 2009). When the outcome of the effect had a >5% chance of being positive and negative, the effect was described as unclear. Median, interquartile range and range of step-to-step changes within each phase were calculated across all ten trials and presented in box and whisker plots.

Results

Ranges of performance (50 m time) and the identified breakpoint steps are presented in Table 2. Only P1 (6.13-6.07 s) and P3 (5.90-5.89 s) improved on their best performance from day 1 to 2. The RMSD between T_{start} identified using TD CM-h or TD shank angles ranged from 0.8-2.1 steps, whilst the RMSD between MV_{start} identified using TD CM-h or TD trunk angles ranged from 1.3-2.3 steps (Table 2). The within-participant ranges of T_{start} steps identified averaged 1.9 steps using TD CM-h and 2.2 steps using TD shank angles. Ranges of MV_{start} steps identified averaged 2.8 steps using TD CM-h and 2.6 steps using TD trunk angles.

****Insert table 2 near here****

To address the second research question, the ranges of T_{start} and MV_{start} steps based on the step-to-step changes in TD CM-h were identified from each participants' best trials and used to sub-divide the whole 50 m sprint into three distinct phases, which had no possible overlap (see shaded areas on Figures 2-4). The initial acceleration phase therefore comprised steps one to three, the transition phase steps six to 13, and the maximal velocity phase steps 17 to 25. T_{start} was associated with step velocities of 6.06 to 7.83 m/s (65 to 77% V_{max}, which was 8.86 to 10.73 m/s), while the MV_{start} was associated with step velocities of 8.19 to 10.07 m/s (92 to 98% V_{max}).

Over the 25 steps, the largest step-to-step changes in step velocity, step length and step frequency (Figure 2) occurred during the initial acceleration phase (i.e. steps 1 to 3), with extremely large step-to-step increases in step velocity and step length and trivial to very large step-to-step increases in frequency compared to the transition and maximal velocity phases. During the transition phase, mean step-to-step increases in step velocity were extremely large, mean increases in step length were large to very large and mean changes in step frequency were trivial to small compared to the maximal velocity phase.

****Insert figure 2 near here****

The initial acceleration phase was characterised by small to very large changes in contact times, flight times, contact distances, flight distances and touchdown distance compared to the transition and maximal velocity phases (Figure 3). During the transition phase, step-to-step changes in contact distances (Figure 3e) plateaued or started decreasing as increases in touchdown distances (0.01 to 0.02 m per step; Figure 3m&n) were equal to or smaller than decreases in toe-off distances (0.01 to 0.03 m per step; Figure 3o&p). During the maximal velocity phase, flight times and flight distances continued to show small step-to-step increases. Mean step-to-step increases in touchdown and toe-off CM-h were very large to extremely large between the initial acceleration and the transition phases and small to large between the transition and maximal velocity phases.

****Insert figure 3 near here****

Step-to-step changes in touchdown CM-angle were most likely large to very large between the initial acceleration phase and both later phases, but most likely only small between the transition and maximal velocity phases (Figure 4). Changes in toe-off CM-angle were most likely moderate to very large between the maximal velocity phase and both preceding phases, and very likely small to very large between the initial acceleration and transition phases.

****Insert figure 4 near here****

Discussion and Implications

Increased understanding of the technical changes associated with different phases in sprinting is important to facilitate the development of technical models of sprinting. Therefore, the aim of this study was to investigate spatiotemporal and kinematic changes between the initial acceleration, transition and maximum velocity phases of a sprint. To address this aim, two research questions were developed.

Firstly, to compare different measures previously proposed in scientific (Nagahara et al., 2014b) and coaching literature (Crick 2014a), the first research question - '*how comparable are the sprint acceleration phases when identified using different measures?'* was addressed. The within-trial RMSD analysis revealed differences up to 2.3 steps between for the T_{start} and MV_{start} steps identified using the different variables. Hypothesis a) that the sprint acceleration phases identified using changes in TD CM-h will align with the phases identified using shank and trunk angles was therefore rejected. Although relatively low, these RMSD step differences are ultimately due to other segments than the shank and trunk changing independently and therefore influencing the TD CM-h. Furthermore, bilateral differences, which have previously been reported in maximal sprinting (Exell, Gittoes, Irwin & Kerwin, 2012) could have contributed to these RMSD step differences. While the within-trial analysis revealed that different T_{start} and MV_{start} steps were identified when using either TD CM-h or touchdown segments angles, both measures did provide similar ranges of T_{start} and MV_{start}

steps across multiple trials. Therefore, using segment angles in applied settings, where the speed of feedback is often an important factor may be an appropriate substitute provided that these data are based on multiple trials (at least three trials per participant). However, since TD CM-h provides a more robust and holistic measure that is more representative of the overall postural changes and changes in CM acceleration, this measure is more appropriate for identifying T_{start} and MV_{start} and was therefore subsequently used to address research question 2.

To understand technical differences between phases, the second research question – '*how do step-to-step progressions of* spatiotemporal and kinematic *variables differ between the initial acceleration, transition and maximal velocity phases?*' was examined. Using TD CM-h, steps one to three were defined as the initial acceleration phase, steps 6-13 the transition phase, and steps 17-25 the maximal velocity phase. Standardised differences in mean between-step increases of the CM-angle between the initial acceleration and transition phases were very large (ES confidence interval: 1.30 to 3.80) for touchdown angles and large (ES confidence interval: 0.33 to 2.31) for toe-off angles. Comparing the transition and maximal velocity phases, standardised differences in mean step-to-step increases of CM-angles were small (ES confidence interval: 0.27 to 0.53) for touchdown angles and very large (ES confidence interval: 1.16 to 2.14) for toe-off angles. Based on this, hypothesis b) that there will be large differences in step-to-step changes of CM-angle between the initial acceleration, transition and maximal velocity phases, was only partially accepted. These changes in touchdown and toe-off CM-angles provide some important insight into the initial acceleration and transition phases.

The more forward-inclined orientation of the participants (i.e. smaller touchdown and toe-off CM-angles; Figure 4a&c) during the initial acceleration phase compared to the transition phase is indicative of the capacity to generate larger net anteroposterior forces (Kugler & Janshen, 2010; Rabita et al., 2015) during this phase. This explains the extremely large step-to-step increases in step velocity during initial acceleration (median 0.88 m/s per step; Figure 2a&b) compared to the transition phase (median 0.24 m/s per step). Additionally, these extremely large increases in step velocity during the initial acceleration phase were achieved through extremely large increases in step length and trivial to very large increases in step frequency, compared to the transition phase. Previous research has reported that across a group of sprinters, performance during the initial acceleration phase is dependent on large increases in step frequency (Nagahara et al., 2014a) and that within athletes, better performances were influenced by larger magnitudes of step frequency throughout the acceleration phase (Nagahara, Mizutani, Matsuo, Kanehisa & Fukunaga, 2017b). Ultimately, the magnitude of the step frequency, which is determined by the sum of contact and flight times, is an important determinant of step velocity. The ability to quickly increase step frequency during the initial acceleration phase (Debaere et al., 2013; Nagahara et al., 2014a) may be an important characteristic of this phase compared to the transition and maximal velocity phases. In the current study, the large step-to-step increases in step frequency (median 0.12 steps·s^{-1} per step; Figure 3a&b) during the initial acceleration phase were due to larger decreases in contact times (median -0.020 s per step; Figure 3a&b) relative to the increases in flight times (median 0.012 s per step; Figure 3a&b). As contact times are related to running velocity (Hunter et al., 2004), shorter contact times are dependent on larger running velocities which can be achieved by applying larger propulsive impulses during preceding steps (Nagahara et al., 2017b). Therefore, as a sprinter's ability to generate larger propulsive forces during the initial acceleration phase increases, their larger change in running velocity will result in larger decreases in contact times which could allow them to achieve larger increases in step frequency.

During the transition phase, further increases in step velocity were mainly due to step-to-step increases in step length, which in turn resulted from further increases in flight distance (Figure 3g). Previous research has demonstrated that flight distance is determined by the anterior and vertical CM velocity at toe-off, the latter of which is also the main determinant of flight time (Hunter et al., 2004). Therefore, as step velocities increase, sprinters need to increase the magnitude of vertical force production to facilitate a decrease in contact times (Figure 3a) without impeding step-to-step increases in CM-h (Figure 3i) and flight times (Figure 3c). However, since a more forward-inclined GRF vector (Rabita et al., 2015; Nagahara, Mizutani, Matsuo, Kanehisa & Fukunaga, 2017a) and a smaller vertical impulse predicts better acceleration performance (Nagahara et al., 2017a), there likely exists an ideal magnitude of vertical force that facilitates increases in step velocity without negatively affecting step frequency through excessively long flight times.

Segmental changes that influence changes in CM-angle can provide an insight into how sprinters adjust force production. During the initial acceleration phase, the relatively large step-to-step increases in touchdown CM-angle, compared to the transition phase, were influenced by increases in shank (median 9° per step) and trunk angles (median 4° per step). These results align with the coaching literature, which suggests that during the initial acceleration phase, experienced sprinters show step-to-step changes in shank angles of between 6 to 8° per step (Crick, 2014b). These increased touchdown variables during the initial acceleration phase could ultimately contribute to the decrease in the anterior forces sprinters can generate during subsequent ground contacts. This may be due to the increases in shank and trunk angles could result in larger touchdown distances, which have been previously linked to larger braking forces (Hunter, Marshall & McNair, 2005). Additionally, the relatively large step-to-step increases in CM-h (Figure 3i&k) and trunk angles (Figure 4e&g) during the initial acceleration phase could influence the increasing toe-off CM-angles (Figure 4c) and therefore the capacity to generate large propulsive forces (e.g. di Prampero et al., 2005; Kugler & Janshen, 2010). Although a decreased touchdown distance has been shown to be beneficial during the first step of a sprint (Bezodis, Trewartha & Salo, 2015), the large magnitude of step-to-step increases in TD variables may ultimately reflect a requirement to generate larger magnitudes of vertical force and therefore flight times (Figure 3c) as a sprint progresses. Previous research from the maximal velocity phase of sprinting suggested that sprinters generate larger vertical forces early during ground contact due to their upright trunk and extended hip and knee joint, which provide increased stiffness at touchdown (Clark & Weyand, 2014). Similarly, during earlier sprint phases, the increasing TD CM-angle (Figure 4a), TD CM-h (Figure 3i) and more extended hip and knee joints due to the increasing TD trunk (Figure 4e) and shank (Figure 4m) angles could increase the capacity to generate vertical force early during ground contact and therefore minimise the loss in CM-h immediately following touchdown.

At toe-off, the CM-angle increased during both the initial acceleration (median 2° per step; Figure 4c&d) and transition phases (median 1° per step; Figure 4c&d). Although smaller CM-angles at toe-off could facilitate larger propulsive force production (Kugler & Janshen, 2010), the step-to-step increases in toe-off CM-angle may be unavoidable given the increases in touchdown CM-angles, CM-h, trunk angles and decreases in contact times. Coaching literature proposed trunk angle and changes in trunk angle as an important factors influencing anterior force production during sprinting (Crick, 2014c), and suggested that better sprinters likely show smaller step-to-step increases in trunk angles (Crick, 2014c). Ultimately, the increasing trunk angle (Figure 4e&g) during the initial acceleration and transition phases may play an important role in influencing the toe-off CM-angle by limiting the anterior rotation of the thigh (Figure 4k) and therefore contribute to the increases in toe-off distances (Figure 3e). This could ultimately contribute to the decreasing magnitude of propulsive forces sprinters can generate as a sprint progresses (e.g. Nagahara et al., 2017a).

Compared to the initial acceleration and transition phases, the maximal velocity phase was characterised by small to negligible step-to-step changes in many spatiotemporal (Figure 2&3) and kinematic variables (Figure 4). At MV_{start}, participants had reached 92-98% of maximal velocity. These results show parity with the British Athletics technical model, which suggests that world-class sprinters reached 95% of maximal velocity at MV_{start} (Crick, 2014c). The participants still showed small increases in step velocity (Figure 2a) which suggests that the participants maintained a positive net anterior impulse during the maximal velocity phase. This was further reflected in the small increases in flight distances (Figure 3g) and therefore step lengths (Figure 2c) which continued throughout the maximal velocity phase. This supports the results by Ae et al. (1992) who reported that step length increases continue throughout a sprint. These results could be explained by the upright trunk and high knee lift, which are associated with this phase of sprinting and allow sprinters a longer path to accelerate their foot down and backwards prior to touchdown. This would contribute to increasing vertical force production earlier during ground contact (Clark & Weyand, 2014) and reduced braking forces (Hunter et al., 2005). The upright posture of sprinters is thought to benefit the mechanics during late swing and early ground contact (i.e. ‘front side mechanics’; Mann, 2007, p. 86) and vertical force production (e.g. Clark & Weyand, 2014) during the maximal velocity phase. However, the increasing trunk angle as a sprint progresses might provide an unavoidable constraint limiting toe-off distances and therefore the magnitude of propulsive forces sprinters can theoretically generate. Therefore, as a sprint progresses through the initial acceleration, transition and maximal velocity phases, sprinters may have a greater ability to manage touchdown rather than toe-off mechanics in an attempt to influence performance.

Despite having five participants in this study, the parity of the results with previous scientific and coaching literature as well as the between-participant consistency regarding the step-to-step changes in the different variables provides confidence in the applicability of this data to investigate changes associated with maximal sprinting. The results presented in the current study provide important insights to increase understanding of the differences between phases in maximal sprinting. Overall, the changing spatiotemporal and kinematic variables through the different phases have important implications for the performance of the sprinters. The changes in CM-h and CM-angle suggest that participants increased vertical force production through changes in touchdown mechanics, while changes in toe-off mechanics suggest an unavoidable limiting feature that dictates decreases in propulsive force production as a sprint progresses. Finally, while breakpoints were identified to define the initial acceleration, transition and maximal velocity phases, this study did not investigate how differences in the location of the breakpoint points between different trials were associated with differences in spatiotemporal and kinematic variables. While the aim of this study was to investigate differences between the phases of a sprint, an investigation of how changes in breakpoints are related to spatiotemporal and kinematic variables may represent a future avenue of research.

Conclusions

The current study has developed an understanding of the technical changes associated with the different phases of a maximal sprint. As long as a sufficient number of trials are available for analysis (at least three), using shank and trunk angles may represent an appropriate measure to detect breakpoint steps in applied settings. However, CM-h represents a more holistic measure of overall postural changes, which links to the centre of mass acceleration, and therefore provides a more robust measure to identify phases during maximal sprinting. This analysis revealed important changes in whole body posture that may be linked to force production, which would ultimately determine the increases in step velocity associated with the initial acceleration phase compared to the transition and maximal velocity phases. These results provide coaches and practitioners with valuable insights into key differences between phases in maximal sprinting.

References

Ae, M., Ito, A. & Suzuki, M. (1992). The men's 100 metres. *New Studies in Athletics*, *7*(1), 47-52.

Batterham, A. M., & Hopkins, W. G. (2006). Making meaningful inferences about magnitudes. *International Journal of Sports Physiology and Performance*, *1*(1), 50-57.

Bezodis, I. N., Kerwin, D. G., & Salo, A. I. (2008). Lower-limb mechanics during the support phase of maximum-velocity sprint running. *Medicine and Science in Sports and Exercise, 40*(4), 707-715.

Bezodis, N. E., Trewartha, G., & Salo, A. I. T. (2015). Understanding the effect of touchdown distance and ankle joint kinematics on sprint acceleration performance through computer simulation. *Sports Biomechanics, 14*(2), 232-245.

Clark, K. P., & Weyand, P. G. (2014a). Are running speeds maximized with simple-spring stance mechanics?. *Journal of Applied Physiology*, *117*(6), 604-615.

Čoh, M. & Tomazin, K. (2006). Kinematic analysis of the sprint start and acceleration from the blocks. *New Studies in Athletics 21*(3), 23-33.

Crick, T. (2014a, November 9). Understanding the performance profiles of sprint events [PDF]. Retrieved from http://ucoach.com/

Crick, T. (2014b, November 9). The Drive Phase. [PDF]. Retrieved from http://ucoach.com/

Crick, T. (2014c, November 9). The Transition, Max Velocity and Speed Maintenance Phases. [PDF]. Retrieved from http://ucoach.com/

de Leva, P. (1996). Adjustments to Zatsiorsky-Seluyanov's segment inertia parameters. *Journal of Biomechanics*, *29*(9), 1223-1230.

Delecluse, C., Van Coppenolle, H., Diels, R., & Goris, M. (1992). A model for the scientific preparation of high level sprinters. *New Studies in Athletics*, *7*(4), 57-64.

Delecluse, C.H., Van Coppenolle, H., Willems, R., Diels, M., Goris, M., Van Leemputte, M., & Vuylsteke, M. (1995). Analysis of the 100 meter Sprint performance as a multi-dimensional skill. *Journal of Human Movement Studies*, *28*, 87-101.

Delecluse, C. (1997). Influence of strength training on sprint running performance. *Sports Medicine, 24*(3), 147 – 156.

di Prampero, P. E., Fusi, S., Sepulcri, L., Morin, J. B., Belli, A., & Antonutto, G. (2005). Sprint running: a new energetic approach. *Journal of Experimental Biology, 208*(14), 2809-2816.

Dick, F. W. (1989). Development of maximum sprinting speed. *Track Coach, 109*, 3475-3480.

Exell, T. A., Irwin, G., Gittoes, M. J., & Kerwin, D. G. (2012). Implications of intra-limb variability on asymmetry analyses. *Journal of Sports Sciences*, *30*(4), 403-409.

Grimshaw, P., Fowler, N., Lees, A., & Burden, A. (2007). Sport and exercise biomechanics (1st ed., pp. 312-316). Abingdon, Oxon: Taylor & Francis Group.

Hedrick, T. L. (2008). Software techniques for two-and three-dimensional kinematic measurements of biological and biomimetic systems. *Bioinspiration & Biomimetics,* 3(3). 034001. doi: 10.1088/1748-3182/3/3/034001.

Hopkins, W. G. (2004). How to interpret changes in an athletic performance test. *Sportscience, 8*, 1–7. Retrieved from sportsci.org/jour/04/wghtests.htm

Hopkins W.G. (2006). Spreadsheets for analysis of controlled trials with adjustment for a predictor. *Sportscience, 10*, 46-50. Retrieved from sportsci.org/2006/wghcontrial.htm

Hopkins, W., Marshall, S., Batterham, A., & Hanin, J. (2009). Progressive statistics for studies in sports medicine and exercise science. *Medicine and Science in Sports and Exercise, 41*(1), 3-12.

Hunter, J. P., Marshall, R.N., & McNair, P. J. (2004). Interaction of Step Length and Step Rate during Sprint Running. *Medicine & Science in Sports & Exercise, 36*(2), 261–271.

Hunter, J. P., Marshall, R. N., & McNair, P. J. (2005). Relationships between ground reaction force impulse and kinematics of sprint-running acceleration. *Journal of applied biomechanics*, *21*(1), 31-43.

Irwin, G. and Kerwin, D.G. (2006). Musculoskeletal work in the longswing on high bar. In: E.F. Moritz and S. Haake (eds.), *The Engineering of Sport 6 Volume 1: Developments for Sports* (pp. 195-200). New York: Springer LLC.

Kugler, F., & Janshen, L. (2010). Body position determines propulsive forces in accelerated running. *Journal of biomechanics*, *43*(2), 343-348.

Mann, R. (2007). The Mechanics of Sprinting and Hurdling. Las Vegas, NV: Author.

Meershoek, L. (1997). Matlab routines for 2-D camera calibration and point reconstruction using the DLT for 2-D analysis with non-perpendicular camera angle [online]. Retrieved from https://isbweb.org/software/movanal.html

Nagahara, R., Naito, H., Morin, J. B., & Zushi, K. (2014a). Association of acceleration with spatiotemporal variables in maximal sprinting. *International journal of sports medicine*, *35*(9), 755-761.

Nagahara, R., Matsubayashi, T., Matsuo, A., & Zushi, K. (2014b). Kinematics of transition during human accelerated sprinting. *Biology Open*, *3*(8), 689–699.

Nagahara, R., Mizutani, M., & Matsuo, A. (2016, July). Ground reaction force of the first transition during accelerated sprinting: a pilot study. In: M. Ae, Y. Enomoto, N. Fujii, & H. Takagi (Eds.), *ISBS 2016. Proceedings of the 34rd International Conference on Biomechanics in Sports* (pp. 859-862). Tsukuba, Japan

Nagahara, R., Mizutani, M., Matsuo, A., Kanehisa, H., & Fukunaga, T. (2017a). Association of sprint performance with ground reaction forces during acceleration and maximal speed phases in a single sprint. *Journal of Applied Biomechanics.* Advance online publication. doi: 10.1123/jab.2016-0356.

Nagahara, R., Mizutani, M., Matsuo, A., Kanehisa, H., & Fukunaga, T. (2017b). Step-to-step spatiotemporal variables and ground reaction forces of intra-individual fastest sprinting in a single session. *Journal of Sports Sciences*. Advance online publication. doi: 10.1080/02640414.2017.1389101

Rabita, G., Dorel, S., Slawinski, J., de Villarreal, E. S., Couturier, A., Samozino, P., & Morin, J. B. (2015). Sprint mechanics in world-class athletes: a new insight into the limits of human locomotion. *Scandinavian Journal of Medicine & Science in Sports, 25*(5), 583-594.

Seagrave, L. (1996). Introduction to sprinting. *New Studies in Athletics, 11*(2), 93- 113.

Volkov, N. I., & Lapin, V. I. (1979). Analysis of the velocity curve in sprint running. *Medicine and Science in Sports and Exercise, 11*(4), 332-337.

Walton, J. (1981). *Close-range cine-photogrammetry: A generalised technique for quantifying gross human motion.* Unpublished Doctoral Thesis. The Pennsylvania State University.

Weyand, P.G., Sternlight, D.B., Bellizzi, M.J., & Wright, S. (2000). Faster top running speeds are achieved with greater ground forces not more rapid leg movements. Journal of Applied Physiology, 89(5), 1991-1999.

Winter, D.A. (2009). *Biomechanics and Motor Control of Human Movement* (4th Edition, p. 86). Hoboken, NJ: John Wiley and Sons, Inc.

Winter, E. M., Abt, G. A., & Nevill, A. M. (2014). Metrics of meaningfulness as opposed to sleights of significance. *Journal of Sports Sciences, 32*(10), 901– 902. doi:10.1080/02640414.2014.895118

Woltring, H. J., & Huiskes, R. (1990). Stereophotogrammetry. In N. Berme, & A. Cappozzo (Eds.), *Biomechanics of human movement: applications in rehabilitation, sports and ergonomics* (pp. 108-127). Worthington, Ohio: Bertec.

Table 1. Participant characteristics.

ID	Age	Gender	Stature [m]	Body Mass [kg]	60 m/100 m PB [s]
P1	27	Male	1.89	89.1	6.99/10.87
P2	20	Male	1.79	73.5	6.80/10.64
P3	19	Male	1.79	72.0	6.86/10.71
P4	20	Female	1.76	69.4	7.65/12.34
P5	25	Female	1.71	63.3	7.61/11.90

Table 2. Ranges of performance times, maximal step velocities and breakpoint steps identified for each participant on each day. RMSD values are presented between T_{start} steps identified using either TD CM-h or TD shank angles, and between MV_{start} steps identified using either TD CM-h or TD trunk angles. Data are based on all available trials for each participant.

Participant	Day	50 m time (s)	Range of maximum Step Velocities (m/s)	**T_{start}**			**MV_{start}**		
				TD CM-h	TD θ_{shank}	TD CM-h vs. TD θ_{shank}	TD CM-h	TD θ_{trunk}	TD CM-h vs. TD θ_{trunk}
P1	1	6.13 – 6.21	9.59 – 9.93	5-7	3-6	1.6	14-17	15-18	1.3
	2	6.07 – 6.15	9.82 – 10.20	3-5	3-6	1.5	13-17	15-17	1.4
P2	1	5.86 – 5.94	10.53 – 10.76	3-5	3-5	1.2	14-15	14-16	1.6
	2	5.98 – 6.01	10.35 – 10.56	3-6	3-6	0.8	13-15	12-16	2.0
P3	1	5.90 – 5.96	10.53 – 10.61	3-4	3-6	2.1	15-17	17-18	2.3
	2	5.89 – 5.94	10.40 – 10.63	4-5	4-6	1.3	14-17	14-17	1.3
P4	1	6.78 – 6.90	8.83 – 9.04	3-5	5	1.1	12-17	14-15	1.6
	2	6.83 – 7.06	8.56 – 8.86	5-6	3-5	1.1	13-16	14-19	1.7
P5	1	6.63 – 6.75	8.99 – 9.15	4-7	4-6	1.1	14-16	13-17	2.0
	2	6.75 – 6.78	8.96 – 9.10	5-7	4-6	0.9	14-17	13-15	1.7
All	1			3-7	3-6	1.5	12-17	13-18	1.8
	2			3-7	3-6	1.1	13-17	12-19	1.7

Note: SV: step velocity, TD CM-h: touchdown centre of mass height, TD θ_{shank}: touchdown shank angles, TD θ_{trunk}: touchdown trunk angles, T_{start}: step representing the start of the transition phase, MV_{start}: step representing the start of the maximal velocity phase.

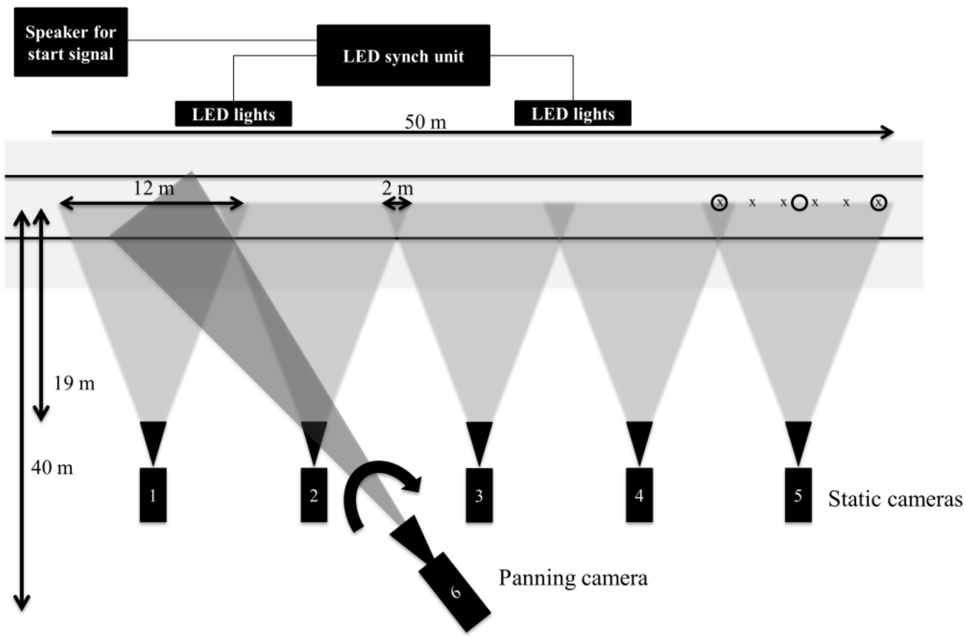

Figure 1. Camera and synchronisation light set-up (not to scale). An example of the camera calibration points for days 1 (O) and 2 (X) are shown in camera 5's field of view. This was repeated for all five static cameras. The direction of travel was from left to right.

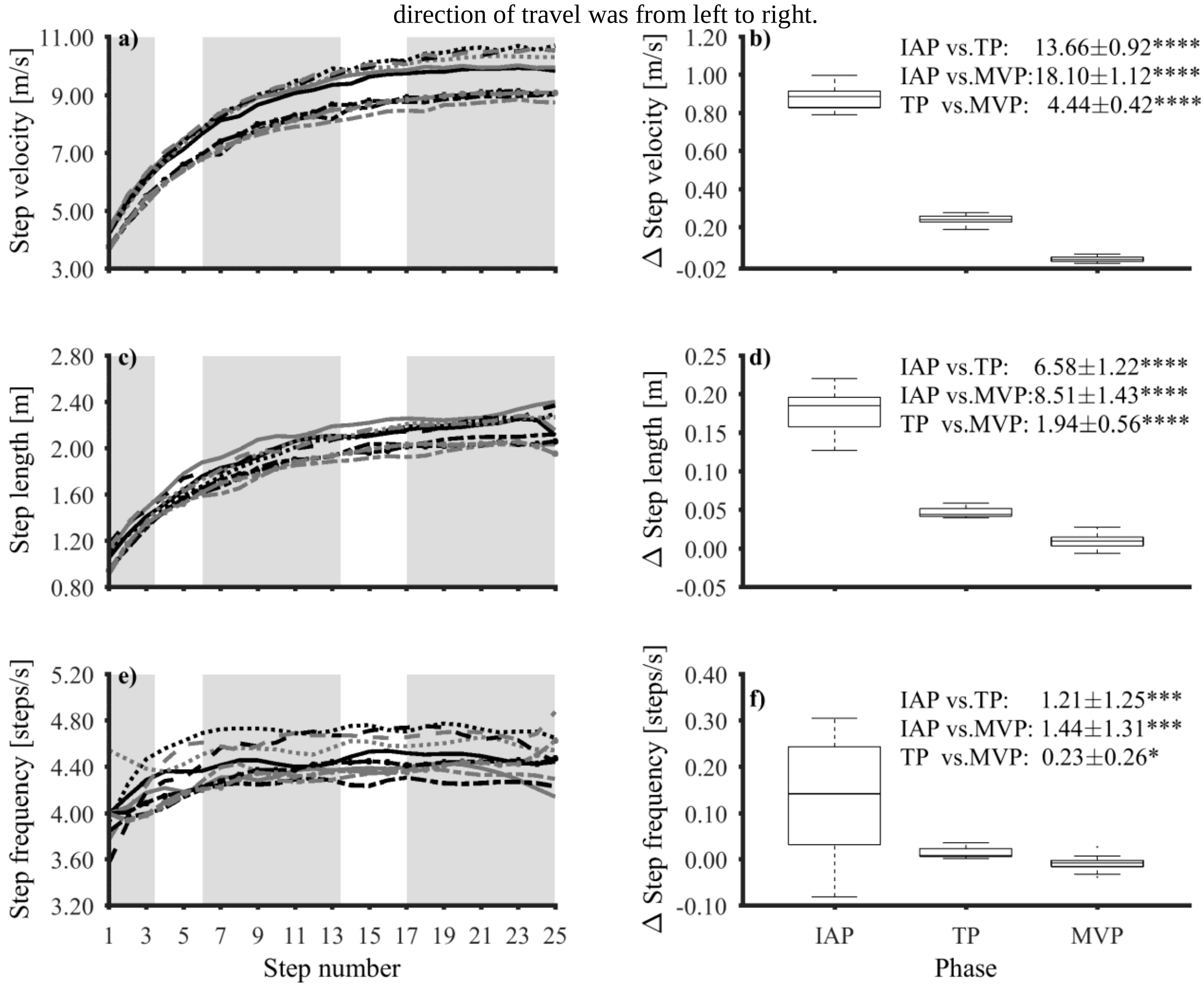

Figure 2. Step-to-step step velocity (a), step length (c) and step frequency (e) profiles of the participants' best 50 m sprints from day 1 (black) and day 2 (grey). Each participant is represented by particular line style. Grey columns highlight the initial acceleration, transition and maximal velocity phases. Box and whisker plots, figures b, d, f show the median, interquartile range and range of between step changes during the initial acceleration,

transition and maximal velocity phases. Magnitude-based inference results presented on figures b, d and f show the mean standardised effect ± 90% confidence interval. The probability that the differences were bigger than the smallest worthwhile change (i.e. 0.20) was defined by: unclear (no stars), possibly (*); likely (**); very likely (***) and most likely (****).

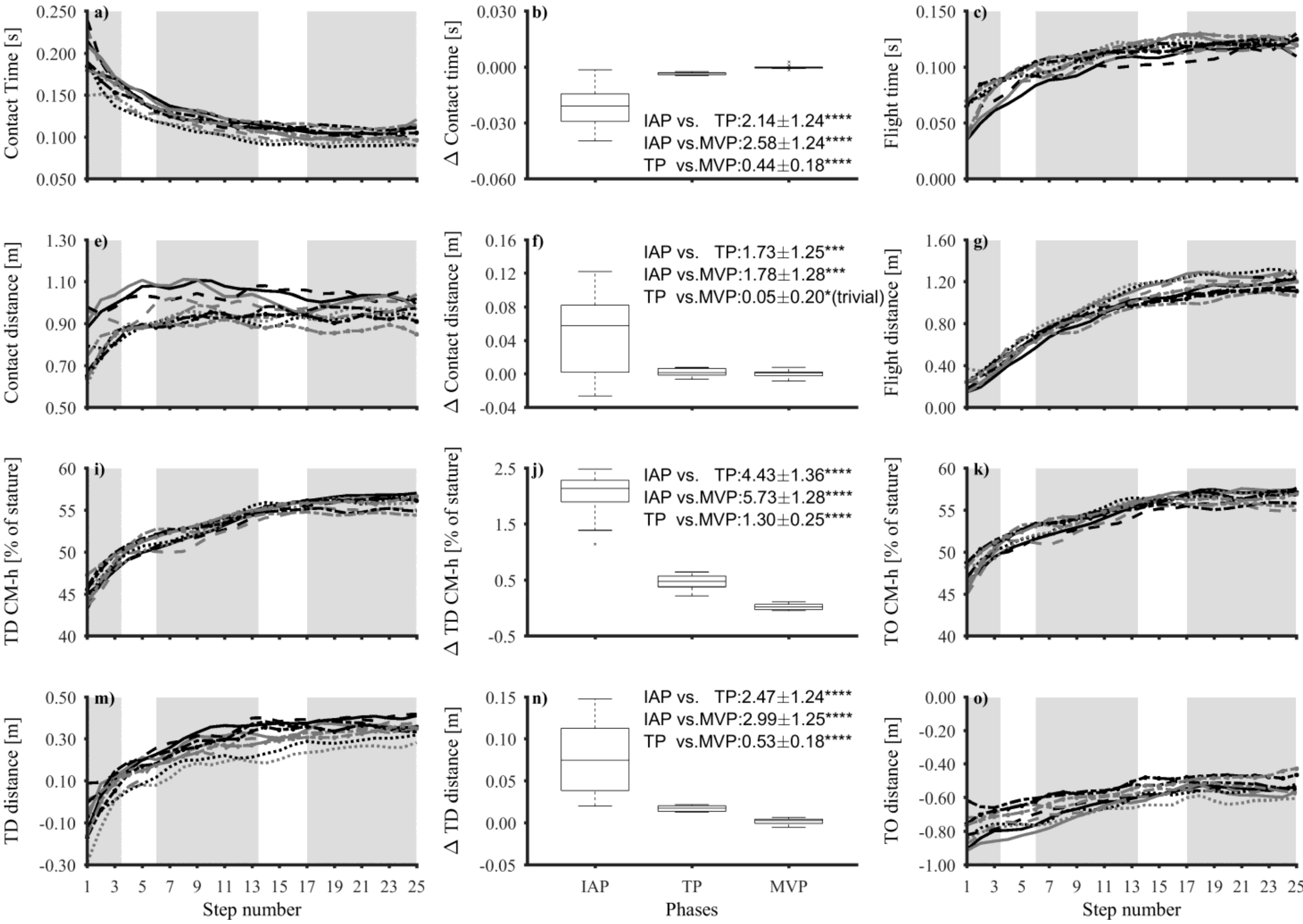

Figure 3. Step-to-step contact times (a), flight times (c), contact distance (e), flight distance (g), TD CM-h (i), TO CM-h (k), TD di
the participants best 50 m sprint from day 1 (black) and day 2 (grey). Each participant is represented by particular line style. Grey c
transition and maximal velocity phases. Box and whisker plots, figures b, d, f, h, j, l, n and p show the median, interquartile range a
the initial acceleration, transition and maximal velocity phases. Magnitude-based inference results presented on figures b, d, f, h, j,
effect ± 90% confidence interval. The probability that the differences were bigger than the smallest worthwhile change (i.e. 0.20) w
(*); likely (**); very likely (***) and most likely (****).

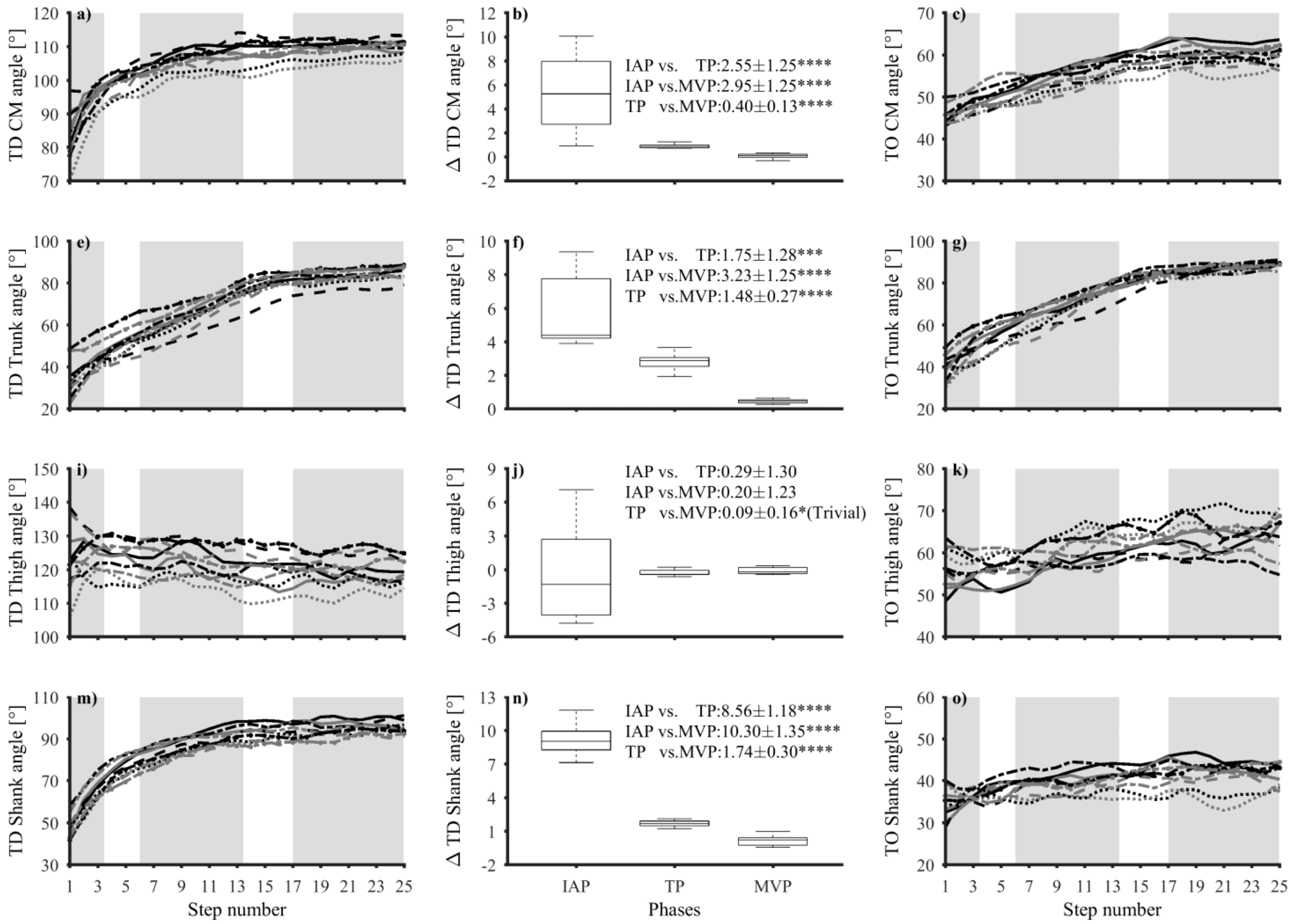

Figure 4. Step-to-step TD CM-angle (a), TO CM-angle (c), TD trunk angle (e), TO trunk angle (G), TD thigh angle (i), TO thigh a angle (o) profiles of the participants best 50 m sprints from days 1 (black) and 2 (grey). Each participant is represented by particula initial acceleration, transition and maximal velocity phases. Box and whisker plots, figures b, d, f, h, j, l, n and p show the median, step changes during the initial acceleration, transition and maximal velocity phases. Magnitude-based inference results presented o mean standardised effect ± 90% confidence interval. The probability that the differences were bigger than the smallest worthwhile (no stars), possibly (*); likely (**); very likely (***) and most likely (****).